THE JOURNAL OF PHYSICAL CHEMISTRY C

Article

pubs.acs.org/JPCC

Intermediates and Dominating Reaction Mechanism During the Early Period of the Methanol-to-Olefin Conversion on SAPO-41

Weili Dai,[†] Michael Dyballa,[‡] Guangjun Wu,[†] Landong Li,*[,†] Naijia Guan,[†] and Michael Hunger*[,‡]

[†]Key Laboratory of Advanced Energy Materials Chemistry of Ministry of Education, Collaborative Innovation Center of Chemical Science and Engineering (Tianjin), Nankai University, Tianjin 300071, China

[‡]Institute of Chemical Technology, University of Stuttgart, 70550 Stuttgart, Germany

ABSTRACT: The formation and evolution of initial reaction intermediates as well as the reaction mechanism during the early period of the methanol conversion on the silicoaluminophosphate SAPO-41 with one-dimensional and 10-numbered ring pore system was elucidated. According to in situ UV−vis spectroscopy, the formation and nature of intermediates formed on the catalysts in the methanol conversion process were monitored. The intermediates remaining on the catalysts after quenching the methanol conversion were determined by ex situ UV−vis, ^{1}H MAS NMR, and ^{13}C MAS NMR spectroscopy, and the reactivity of these species was investigated by adsorption of ammonia and subsequent solid-state NMR spectroscopy. The above-mentioned spectroscopic studies gave a detailed mechanistic insight into the induction period of the methanol conversion on SAPO-41. Monoenylic carbenium ions, being the dominating species during the initial period of the methanol conversion, were rapidly formed and gradually transferred to dienylic carbenium ions, benzene-based carbenium ions, and trienylic carbenium ions, in addition to three-ring compounds and dienes with different chain lengths. On the basis of these spectroscopic observations and the catalytic results, the olefin-based reaction cycle is disclosed to be the dominating reaction mechanism in the initial period of the methanol conversion on SAPO-41.

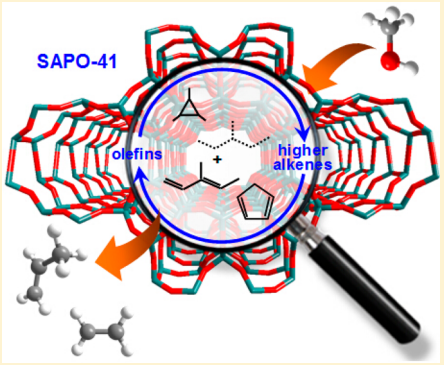

1. INTRODUCTION

With the increasing requirement of light olefins and the limited oil resources, methanol to olefin (MTO) conversion over acidic zeolite catalysts, as an alternative route to gain light olefins, has attracted much attention, since it was first discovered in the 1970s.[1−5] Considering the important role of the light olefins, e.g., ethene and propene, in the global oil chemical enterprise, understanding of the mechanism of MTO conversion is extremely important for both fundamental research and commercial application. As a complex process of MTO conversion, clarification of its mechanism is becoming an intellectually challenging topic. Among many possible mechanisms, an indirect hydrocarbon pool mechanism is widely agreed in the MTO conversion.[6−10] The essential feature of the hydrocarbon pool mechanism is that methanol can react with the hydrocarbon species formed in the catalyst and induce a sequence of steps leading to primary olefins and regeneration of the hydrocarbon species in a closed cycle.[10]

According to the hydrocarbon pool mechanism, polymethylbenzenes and their protonated forms have been established as the active hydrocarbons in SAPO-34 and H-BEA catalysts with large cages.[11−16] Recent experimental and theoretical work proposed that olefins may act as another kind of active hydrocarbon pool species, particularly in the zeolites with medium-pore structure, e.g., H-ZSM-5 zeolite with a three-dimensional (3-D) 10-ring pore structure and H-ZSM-22 zeolite with one-dimensional (1-D) 10-ring pore system.[17−20] This leads to the establishment of the dual-cycle mechanism, i.e., the aromatics-based cycle produces ethene and methylbenzenes, while the olefin-based methylation/cracking cycle produces C_{3+} olefins.[21,22] Considering that both aromatics and olefins exist in zeolite pores, the corresponding olefin- and aromatic-based routes operate on a competing basis. For example, the small 8-numbered ring windows of H-SAPO-34 hinder the diffusion of C_{5+} hydrocarbons from the larger chabasite cages, leading to the aromatic-based cycle dominating the MTO conversion.[6−10] On the contrary, the olefin-based cycle dominates in the H-ZSM-22 zeolite with a 1-D 10-numbered ring pore system, which is too small for the formation of polymethylbenzenes.[23−26] In H-ZSM-5 zeolite with 3-D 10-numbered ring pore structure, both cycles contribute to the product distribution.[27]

With the aid of ^{12}C/^{13}C methanol-switching experiments and cofeeding methanol and olefins/aromatics, the dominating catalytic cycle of the MTO conversion was verified for different zeolites, and the aromatic- and olefin-based cycles could be propagated to different extents depending on the reaction conditions.[22,27−30] By combining spectroscopic observations and theoretical calculations, very recently we demonstrated that the olefin-based catalytic cycle plays a great role during the

Received: November 28, 2014
Revised: January 9, 2015
Published: January 14, 2015

DOI: 10.1021/jp5118757
J. Phys. Chem. C 2015, 119, 2637−2645

initial period of the methanol conversion on H-SAPO-34.[31] However, to the best of our knowledge, no direct experimental evidence has been disclosed for the initial intermediates in MTO catalysts with a 1-D pore system, e.g., SAPO-41, which is, therefore, the goal of the present work.

Silicoaluminophosphate SAPO-41 with 10-numbered ring pore structure and moderate acidity has been studied in the MTO conversion, and the olefin-based catalytic cycle was verified as the dominating reaction mechanism in our previous studies.[32,33] However, the details of the reaction mechanism in the early period of the methanol conversion over this material are yet missing. The present work focuses on verification of the initial species in the early period of the methanol conversion on SAPO-41 zeolite by combining spectroscopic and catalytic investigations. Applying in situ UV−vis, ^{1}H MAS NMR, and ^{13}C MAS NMR spectroscopy, we obtained detailed mechanistic insight into the early period of the methanol conversion over SAPO-41.

2. EXPERIMENTAL SECTION

2.1. Sample Preparation and Characterization. SAPO-41 was synthesized via the hydrothermal route following the procedure described in our former report.[33] X-ray diffraction (XRD) patterns of the calcined SAPO-41 sample were determined on a Bruker D8 diffractometer with Cu Kα radiation (λ = 1.5418 Å) at 5−50°. Solid-state nuclear magnetic resonance (NMR) experiments were recorded on Bruker Avance III 400WB spectrometer at resonance frequencies of 400.1, 104.3, 79.5, and 161.9 MHz for ^{1}H, ^{27}Al, ^{29}Si, and ^{31}P nuclei, respectively. Sample spinning rates of 8 kHz for ^{1}H, ^{27}Al, and ^{31}P nuclei and 4 kHz for ^{29}Si nuclei and the parameters described elsewhere were used.[31]

2.2. Catalytic Investigations. The MTO conversion was performed in a fixed-bed reactor at atmospheric pressure as described in the literature.[31] Typically, 0.1 g of sample with a sieve fraction of 0.25−0.5 mm was placed in a stainless steel reactor (5 mm i.d.) and activated under flowing N_2 at 400 °C for 1 h and then decreased to the desired temperature. Pure ^{13}C-methanol with a flow of 0.5 mL/h (WHSV = 4 h^{-1}) was introduced into the catalyst by the carrier gas (N_2). The reaction products were analyzed by an online gas chromatograph equipped with a flame ionization detector and a capillary column Plot Q to separate the product. The temperature of the column was maintained at 40 °C for 7 min, increased to 200 °C with a rate of 10 °C/min, and then maintained at 200 °C for 4 min.[33]

2.3. In Situ and ex Situ UV−Vis Studies of the MTO Conversion on SAPO-41. The nature of organic intermediates formed on the catalysts during the MTO conversion was in situ monitored by UV−vis spectroscopy as described in ref 31. After MTO conversion, the organic compounds occluded inside the catalyst were investigated by ex situ UV−vis spectroscopy. UV−vis spectra were recorded in the diffuse reflection mode in the range of 200−600 nm using an AvaSpec-2048 fiber optic spectrometer, an AvaLight-DH-S deuterium light source by Avantes, and a glass fiber reflection probe HPSUV1000A by Oxford Electronics. Before starting the MTO reaction, the glass fiber reflection probe was placed in the fixed-bed reactor on the top of the catalyst with a gap of ca. 1.0 mm. Reference UV−vis spectra of catalysts were recorded at the reaction temperature prior to starting the methanol flow.[31]

2.4. Solid-State MAS NMR Characterization of Organic Compounds. The organic compounds formed and occluded inside the used SAPO-41 catalysts were determined by ^{1}H MAS NMR and ^{13}C MAS NMR spectroscopy utilizing a Bruker Avance III 400WB spectrometer. For the ^{1}H MAS NMR measurements, a resonance frequency of 400.1 MHz, with $\pi/2$ single pulse excitation, a repetition time of 10 s, and a sample spinning rate of 8.0 kHz by a 4.0 mm MAS NMR probe were used, while for ^{13}C MAS NMR measurements a resonance frequency of 100.6 MHz with $\pi/2$ single pulse excitation, a repetition time of 20 s, and a sample spinning rate of 12.0 kHz by a 4.0 mm MAS NMR probe were used.[31]

3. RESULTS AND DISCUSSION

3.1. Physicochemical Properties of SAPO-41. The XRD pattern of the calcined SAPO-41 sample shows typical diffraction lines corresponding to the AFO framework structure,[33] which indicates that pure SAPO-41 without any impurity phases was obtained (not shown). ^{1}H, ^{27}Al, ^{29}Si, and ^{31}P MAS NMR spectra of the calcined SAPO-41 samples (not shown) are similar to our previous reports,[33] indicating that the Brønsted acid sites and textual properties of the SAPO-41 material are well maintained after calcination.

3.2. Catalytic Performance of SAPO-41 in the MTO Conversion. The catalytic performance of the SAPO-41 catalyst in MTO conversion is shown in Figure 1. The methanol conversion at various reaction temperatures with a time-on-stream (TOS) of 5 min was first tested and presented in Figure 1A. At 300 °C, nearly no methanol conversion can be observed. With the increase of the reaction temperature from 325 to 425 °C, the methanol conversion increases from 4.1% to 100% and the production of olefins occurs.

To investigate the initial intermediates formed in the methanol conversion on SAPO-41 the catalytic performance at a reaction temperature of 350 °C was investigated in detail. In Figure 1B, the time dependence of the methanol conversion and product selectivity up to TOS = 60 min are shown. Obviously, an induction period and a rapid deactivation of the SAPO-41 catalyst occur, which start already at TOS = 15 min, similar to the case of SAPO-34.[31] Because of using WHSV = 4.0 h^{-1}, the lifetime of the SAPO-41 catalyst in the present study is much shorter than in our previous investigations performed with WHSV = 1.0 h^{-1}.[32,33] Concerning the product distributions, higher selectivities to propene (30%), butenes (20%), and pentenes (12%) than ethene (5.0%) occur after the first 5 min. With the progress of the MTO conversion, the selectivity to the above-mentioned products keeps stable, while the selectivity to aromatics and other products, including gasoline-range hydrocarbons, gradually increases. According to the dual-cycle mechanism, the aromatics-based cycle forms ethene and methylbenzenes and the olefin-based methylation/cracking cycle produces C_{3+} olefins.[21,22] Therefore, it can be concluded that the olefin-based cycle plays a key role during the early period of the methanol conversion on SAPO-41.

3.3. In Situ UV−Vis Studies of the Methanol Conversion on SAPO-41. In situ UV−vis spectroscopy was utilized to study the nature of organic intermediates formed in the methanol conversion process over SAPO-41. Figure 2 shows the in situ UV−vis spectra of SAPO-41 catalyst in the methanol conversion process at 325−400 °C and in steps of 5 min. At the reaction temperatures of 325 and 350 °C and during the first 2 min, i.e., during the early period of methanol conversion, a dominating band occurs at 290 nm. With further

DOI: 10.1021/jp5118757
J. Phys. Chem. C 2015, 119, 2637−2645

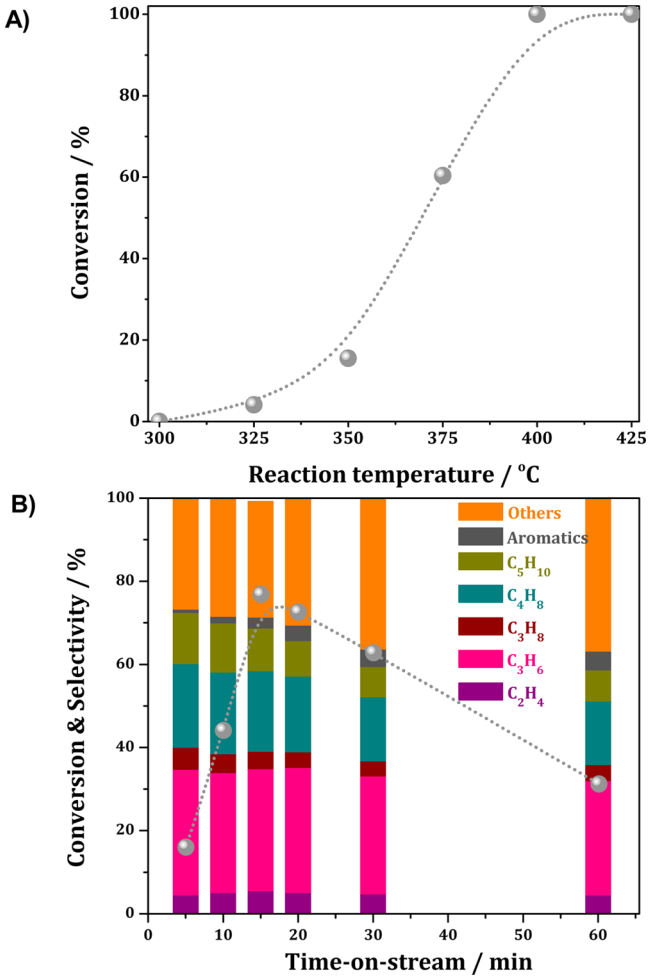

Figure 1. Methanol conversion (gray dots) on SAPO-41 at TOS = 5 min for different reaction temperatures (A), and methanol conversion (gray dots) and product selectivities (colored columns) obtained during the MTO conversion at 350 °C up to TOS = 60 min (B).

progress of the methanol conversion (TOS > 2 min), additional weak bands appear at 245, 370, and 445 nm and the intensities of these bands increase rapidly. On the basis of the former reports, the bands at 245, 290, 370, and approximately 445 nm are attributed to dienes (e.g., cyclopenta- and cyclohexadienes), monoenylic carbenium ions (e.g., cyclopentenyl and cyclohexenyl cations) or polyalkylaromatics, dienylic carbenium ion, and trienylic carbenium ions, respectively.[31,36−38] In contrast to previous UV−vis studies on H-SAPO-34 catalysts under similar methanol conversion conditions,[31] no band attributed to benzene-based carbenium ions appeared at 390 nm. These observations indicate that monoenylic carbenium ions (290 nm) play a major role in the initial stage of the methanol conversion on SAPO-41. Subsequenly, these monoenylic carbenium ions react with olefins to dienylic (370 nm) and trienylic carbenium ions (445 nm) forming the hydrocarbon pool in the working catalysts.

At reaction temperatures of 375 and 400 °C, a quick transformation of the carbenium ions occurs and the band of dienylic carbenium ions (370 nm) is rapidly overlapped by the bands of benzene-based carbenium ions (390−400 nm) and trienylic carbenium ions (445 nm). Meanwhile, much more dienes (245 nm) are formed. These results indicate that the induction period of MTO conversion is very short and the carbenium ions exhibit high reactivity at higher reaction temperatures of 375 and 400 °C compared to the situation at 325 and 350 °C.

In order to get more information on the fate of the organic intermediates during the MTO conversion upon longer TOS, further in situ UV−vis studies focused on the reaction temperature of 350 °C (Figure 3). The concentrations of all organic compounds, reflected as the intensities of the corresponding UV−vis bands, change strongly with the progress of methanol conversion. The bands of dienes, monoenylic carbenium ions, and polyalkylaromatics are slightly shifted to the ranges of 225−245 and 275−290 nm. These observations indicate that carbon chain growth or cyclization reactions take place.[37] Additionally, dienylic carbenium ions (370 nm) are gradually transformed to benzene-based carbenium ions (390−400 nm)[39] and trienylic carbenium ions (445 nm). This observation indicates that polymethylbenzenium cations are formed from monoenylic and dienylic carbenium ions. After the formation of polymethylbenzenium cations, the aromatic-based cycle begins to contribute to the MTO reaction, which proceeds via methylation of aromatics and subsequent elimination of side alkyl chains to produce light olefins as reaction products.

3.4. Solid-State MAS NMR Studies of the Intermediates Formed during Methanol Conversion over SAPO-41. After recording the in situ UV−vis spectra, methanol conversion was stopped and SAPO-41 catalysts after MTO conversion were transferred from the fixed-bed reactor into NMR rotors without contact to air for solid-state ^{1}H and ^{13}C NMR measurements.

Figure 4 shows the ^{1}H MAS NMR spectra of the used SAPO-41 catalysts after methanol conversion at various reaction temperatures for 5 min and recorded with and without ammonia loading. ^{1}H MAS NMR spectra of the SAPO-41 catalyts after MTO reaction at 325 and 350 °C are dominated by the signals at 3.5−4.2 ppm. The main signal at 3.6 ppm is attributed to bridging OH groups,[31] and the narrower and significantly weaker signals at 3.5 and 3.7 ppm may be attributed to methyl groups of single or multiple methanol molecules, adsorbed on SAPO-41.[40] The broad signal appearing at 12.2 ppm is caused by the hydroxyl protons involved in hydrogen bonds between methanol molecules and the zeolite framework.[31,41] Besides the above-mentioned signals, some weak signals appear at 0.1, 0.6−2.3, and 5.5−7.6 ppm. The weak signal at 0.1 ppm hints to the presence of AlOH groups, which may be formed by reaction water coordinated to framework aluminum species.[33] The three weak signals at 0.6, 0.8, and 0.9 ppm are attributed to organic three-ring compounds, e.g., trimethylcyclopropane (δ_{1H} = 0.56 and 0.89 ppm), which can be formed on SAPO-41 catalyst in short reaction time.[41,42] Additional signals occur at 5.5−7.6 ppm that can be assigned to alkenes and aromatics. These spectral ranges are also typical for nonbranched and branched dienes, such as cyclopentadiene (δ_{1H} = 2.80, 6.14, and 6.22 ppm), 2,4-hexadiene (δ_{1H} = 1.7, 5.5−5.9 ppm), and 3-methyl-1,3-pentadiene (δ_{1H} = 1.8, 5.6−6.5 ppm).[33,41]

Upon a further increase of the reaction temperature ($T \geq$ 350 °C), more three-ring compounds (δ_{1H} = 0.6−0.9 ppm) and olefinic/aromatic species (δ_{1H} = 5.5−7.6 ppm) were formed. Simultaneously, the weak signals due to methyl groups of methanol at 3.5−3.7 ppm gradually disappear, which implies that more methanol molecules are converted to olefins, which is in line with the catalytic results (Figure 1). For H-SAPO-34

DOI: 10.1021/jp5118757
J. Phys. Chem. C 2015, 119, 2637−2645

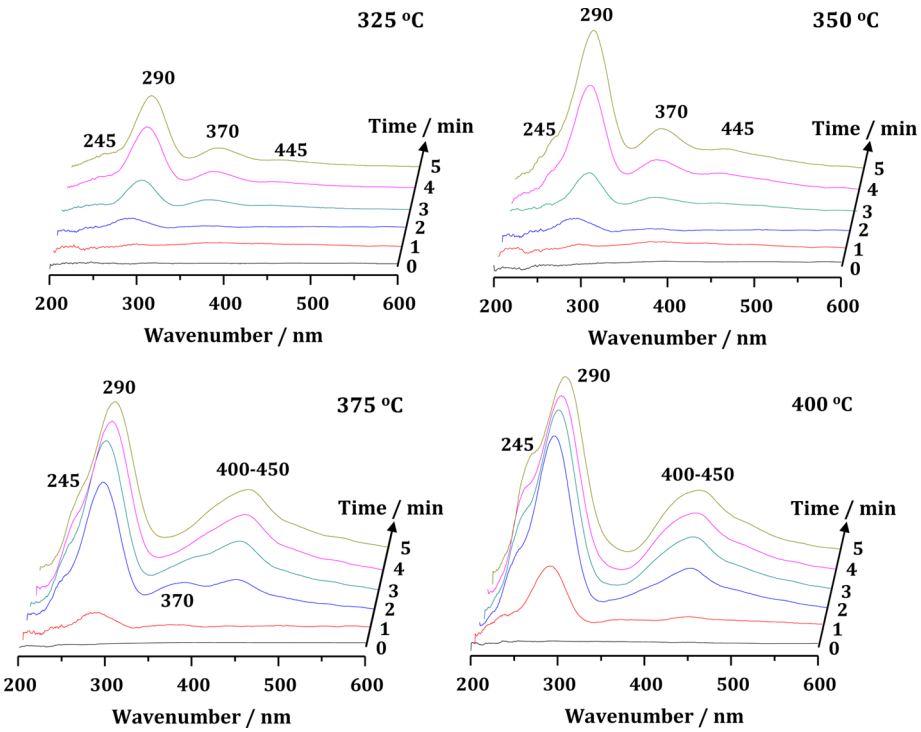

Figure 2. In situ UV−vis spectra recorded during the MTO conversion on SAPO-41 up to TOS = 5 min at reaction temperatures of 325−400 °C.

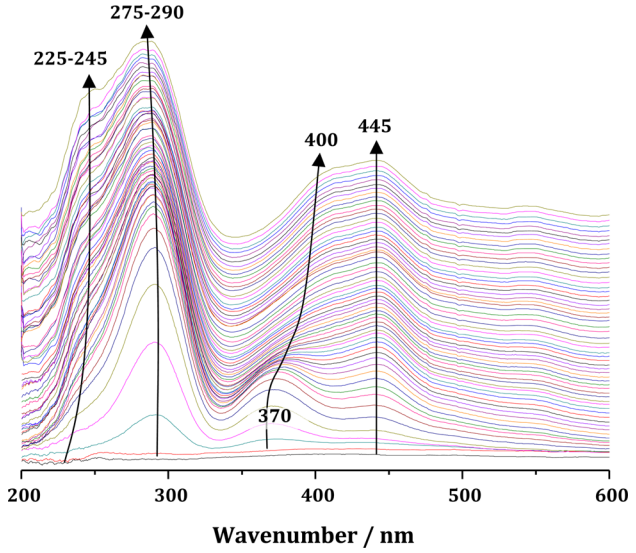

Figure 3. In situ UV−vis spectra recorded during the MTO conversion on SAPO-41 up to TOS = 60 min at the reaction temperature of 350 °C.

applied as MTO catalysts, a broad weak ^{1}H MAS NMR signal at δ_{1H} = 8−9 ppm attributed to monoenylic carbenium ions, e.g., five-ring or six-ring carbenium ions, can be observed at low reaction temperature and short reaction time.[31] The absence of these signals in the ^{1}H MAS NMR spectra of SAPO-41 applied as MTO catalyst (Figure 4, left) may indicate that these carbenium ions, occurring at 290 nm in the UV−vis spectra (Figure 2), are not stable. Therefore, these compounds cannot be observed by ^{1}H MAS NMR spectroscopy after quenching the MTO reaction.

To investigate the reactivity of the intermediates formed on SAPO-41 during the MTO conversion, ^{1}H MAS NMR spectroscopic studies of used SAPO-41 catalysts upon ammonia loading were performed (Figure 4, right). After ammonia loading, additional ^{1}H MAS NMR signals appeared at 6.7, 3.4, and 2.6 ppm. The signal at 6.7 ppm can be attributed to the ammonium ions, caused by protonation of ammonia on Brønsted acid sites.[32] The signals appearing at 3.4 and 2.6 ppm are due to the monosubstituted secondary amines, which were caused by reaction of ammonia with alkenes and alkylbenzene, probably in their carbenium or alkoxy states. Possible examples are mono- to pentamethylphenylamine (δ_{1H} = 3.49−3.40 ppm), methylamine (δ_{1H} = 2.46 ppm), ethylamine (δ_{1H} = 2.61 ppm), propylamine (δ_{1H} = 2.67 ppm), or secondary NH_2 groups at larger alkane chains (δ_{1H} = 2.50 ppm).[41,42] The observed amines indicate the high activity of the organic compounds, which can react with the adsorbed ammonia. Since no carbenium ions (δ_{1H} = 8−9 ppm) could be observed in the ^{1}H MAS NMR spectra before ammonia loading (Figure 4, left), alkoxy species formed by reaction of methanol or carbenium ions with Brønsted acid sites may be the main states of these organic compounds in the present study.

Interestingly, an additional ^{1}H MAS NMR signal appearing at 4.7 ppm could be observed after ammonia loading. An assignment of this signal to bridging OH groups can be excluded, since these surface species react with ammonia, and their signal would disappear after ammonia loading (see Figure 7, top and right). According to our previous study,[43] the signal at 4.7 ppm may be due to dienes with short chain, such as 2,3-dimethyl-1,3-butadiene (δ_{1H} = 4.9 and 1.9 ppm). In comparison with the findings for SAPO-34 applied as MTO catalysts, the phenylammonium ions (δ_{1H} = 5.1 ppm)[43−46] are absent in the ^{1}H MAS NMR spectra of ammonia-loaded SAPO-41. This means that the benzene-based carbenium ions, occurring at 390−400 nm in the UV−vis spectra (Figure 2), are also not stable and cannot be observed by ^{1}H MAS NMR spectroscopy after quenching the MTO reaction.

DOI: 10.1021/jp5118757
J. Phys. Chem. C 2015, 119, 2637−2645

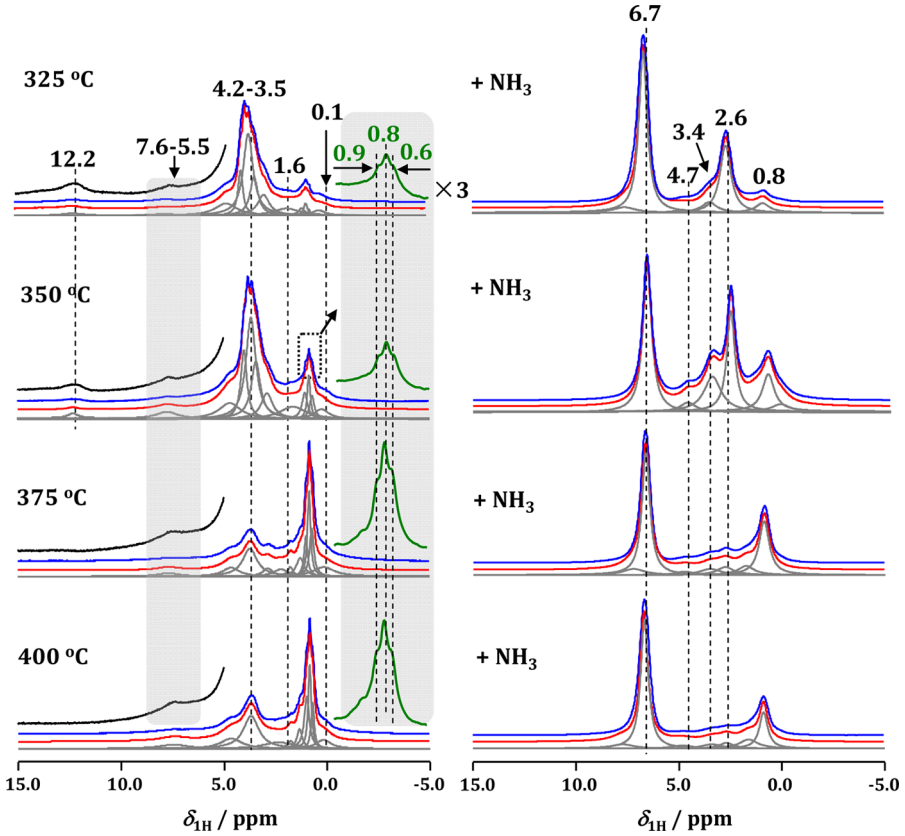

Figure 4. ^{1}H MAS NMR spectra of SAPO-41 catalysts obtained after MTO conversion at various reaction temperatures for TOS = 5 min and recorded before (left) and after (right) adsorption of ammonia. From top to bottom, experimental spectra, simulated spectra, and signal components utilized for simulation are shown.

To confirm the above-mentioned ^{1}H MAS NMR assignments of the initial hydrocarbons formed over SAPO-41 in the initial stages of the methanol conversion, ^{13}C NMR spectroscopy was performed. Figure 5 shows the ^{13}C MAS NMR spectra of the used SAPO-41 catalysts obtained after MTO conversion for 5 min at different reaction temperatures.Consistent with the ^{1}H MAS NMR spectroscopic results, the adsorbed methanol (δ_{13C} = 50 ppm), DME (δ_{13C} = 60 ppm), and surface methoxy species (δ_{13C} = 56 ppm) are observed as predominant intermediates formed on the SAPO-41 catalyst after methanol conversion at 325 and 350 °C.[47] Besides the above-mentioned strong signals, several weak peaks occur at 9−46 and 120−145 ppm, caused by alkyl groups and alkenes as well as aromatics, respectively.[44] Weak signals at ca. 9 and 14 ppm attributed to organic three-ring compounds, e.g., trimethylcyclopropane (δ_{13C} = 9.8 and 14.7 ppm), also appear in the ^{13}C MAS NMR spectrum,[48] which are in line with the results of ^{1}H MAS NMR spectroscopy (see Figure 4).

When the reaction temperature increases above 350 °C, more three-ring compounds (9−14 ppm) and alkenes as well as aromatics (120−145 ppm) are formed. Simultaneously, the signals of DME and methoxy species at 60 and 56 ppm disappear, which are coincident with the ^{1}H MAS NMR spectra shown in Figure 4.

After ammonia loading, new signals appear at 24.8 ppm, along with the decrease in the intensity of surface methoxy species at 56.4 ppm. These new signals can be assigned to methylamine/protonated methylamine,[47] (Figure 5, right), which fit well with the results of ^{1}H MAS NMR spectroscopy (see Figure 4, right). However, no ^{13}C MAS NMR signals due

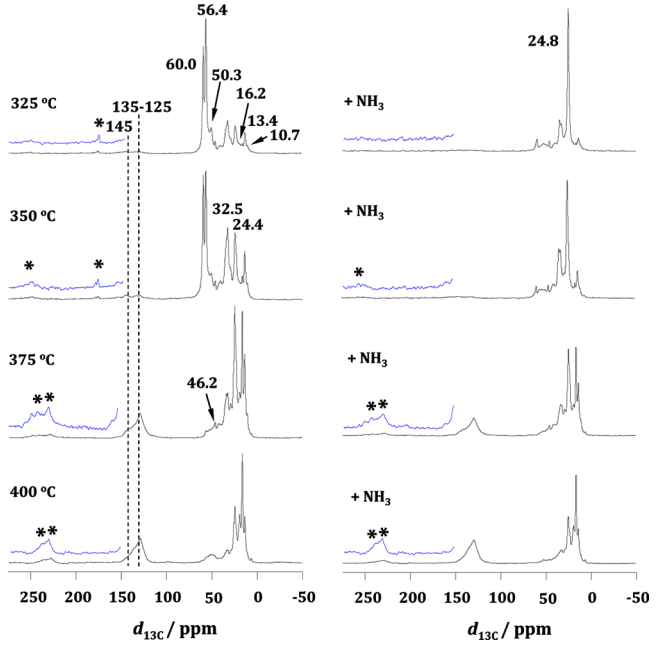

Figure 5. ^{13}C MAS NMR spectra of SAPO-41 catalysts obtained after MTO conversion at various temperatures for TOS = 5 min and recorded before (left) and after (right) adsorption of ammonia.

to five-membered ring cations (polymethylcyclopentenyl cations) and six-membered ring cations (polymethylbenzenium cations) could be observed at 190−210 and 240−250 ppm, respectively.[31,49,50] Compared with the results of in situ UV−vis

DOI: 10.1021/jp5118757
J. Phys. Chem. C 2015, 119, 2637−2645

and ^{1}H MAS NMR spectroscopy, the absence of the ^{13}C MAS NMR signals of carbenium ions may be caused by their instability. They do not exist in their carbenium states after quenching the MTO reaction, which is again coincident with the results of ^{1}H MAS NMR spectroscopy (see Figure 4).

To confirm the above-mentioned statement of the absence of carbenium ions in ^{1}H and ^{13}C MAS NMR spectra, ex situ UV−vis spectroscopy of the used SAPO-41 catalysts was also performed, and the results are shown in Figure 6. In contrast to

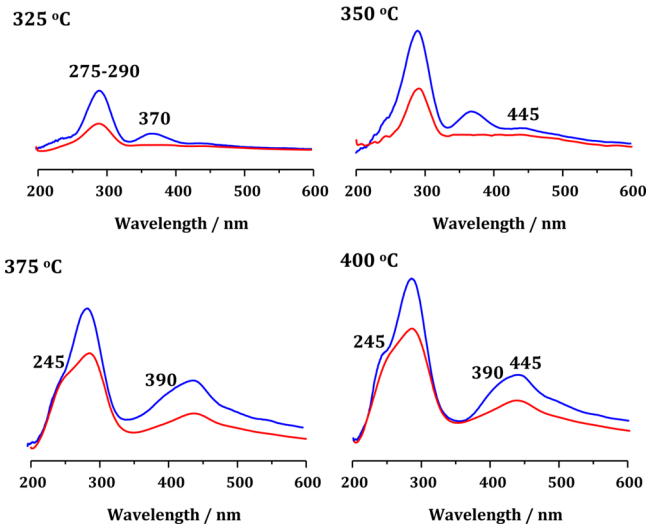

Figure 6. In situ (blue) and ex situ (red) UV−vis spectra of SAPO-41 catalysts obtained after MTO conversion at various temperatures for TOS = 5 min.

the in situ UV−vis spectra (Figure 6, blue), the band intensities at 290 (monoenylic carbenium ions), 370 (dienylic carbenium ions), and 445 nm (trienylic carbenium ions) in the ex situ UV−vis spectra are strongly decreased or disappeared (Figure 6, red). These results confirm that the carbenium ions formed during the MTO conversion are not stable in SAPO-41. As a result, these compounds cannot be observed in ^{1}H MAS NMR, ^{13}C MAS NMR, and ex situ UV−vis spectra recorded after quenching the MTO conversion.

For clarifying the fate of the observed organic species in the initial period of the methanol conversion on SAPO-41, catalysts gained after reaction times of up to 60 min at a reaction temperature of 350 °C were studied by ^{1}H MAS NMR spectroscopy before and after ammonia loading (see Figure 7). The ^{1}H MAS NMR spectrum of fresh SAPO-41 is dominated by a sharp signal at 3.6 ppm due to Brønsted acid sites, which react with ammonia to ammonium ions, leading to a signal at 6.7 ppm (Figure 7, top). After the MTO conversion (TOS ≥ 5 min), methoxy groups (3.5−4.0 ppm), three-ring compounds (0.6−0.9 ppm), and olefins and aromatics (5.5−7.6 ppm) appeared. With the progress of the methanol conversion, the signals of Brønsted acid sites and methoxy groups obviously decrease while the intensities of the signals due to olefins and aromatics gradually increase. In addition, the signals at 0.6 and 0.9 ppm, caused by three-ring compounds, disappear or overlap with the signal at 0.8 ppm. Furthermore, the signals at 4.7 ppm, caused by dienes with short chains, gradually decrease after ammonia loading with progress of the MTO conversion. This finding implies that three-ring compounds as intermediates can be transferred to other organic compounds and, therefore, cannot be observed upon increasing TOS.

3.5. Mechanism of the Early Period of Methanol Conversion on SAPO-41. In the present work, UV−vis as well as ^{1}H and ^{13}C MAS NMR spectroscopy combined with the catalytic studies were applied to investigate the initial intermediates and their evolution process during the early period of the methanol conversion on SAPO-41.

As demonstrated by in situ UV−vis spectroscopy, monoenylic carbenium ions or polyalkylaromatics as the dominating intermediates are rapidly formed in the early period of methanol conversion at low reaction temperatures (325 and 350 °C). Interestingly, benzene-based carbenium ions, observed in the induction period of the methanol conversion on H-SAPO-34, were not observed for SAPO-41. This finding indicates that monoenylic carbenium ions play an important role in the early period of methanol conversion on SAPO-41, i.e., the olefin-based reaction cycle is the dominating reaction mechanism in this situation.

With the further progress of the methanol conversion on SAPO-41, dienylic carbenium ions and trienylic carbenium ions are gradually formed, together with monoenylic carbenium ions, and a transformation from dienylic carbenium ions to benzene-based carbenium ions occurs, as evidenced by in situ UV−vis spectroscopy. Several additional compounds, e.g., methylcyclopropane and dienes, can be detected by ^{1}H and ^{13}C MAS NMR spectroscopy of SAPO-41 obtained after short TOS. These species, serving also as intermediates, are more stable than carbenium ions and support the olefin-based reaction cycle during the early period of the methanol conversion on SAPO-41.

4. CONCLUSION

For elucidating the initial organic species and verifying the reaction mechanism in the early period of the methanol conversion on SAPO-41, in situ UV−vis spectroscopy was applied to investigate the formation process of the organic species. The organic compounds remaining on SAPO-41 after quenching the MTO reaction were measured via ex situ UV−vis and ^{1}H and ^{13}C MAS NMR spectroscopies. On the basis of these spectroscopic studies, the initial organic species and the reaction mechanism in the early period of the methanol conversion on SAPO-41 can be described as follows.

(i) Three-ring compounds (NMR) and dienes with different chain length (UV−vis, NMR) occur as very early reaction intermediates.
(ii) Monoenylic carbenium ions, as the dominating intermediates in the early period of the methanol conversion, are rapidly formed (UV−vis).
(iii) After the formation of monoenylic carbenium ions, dienylic carbenium ions appear and are gradually transferred to benzene-based carbenium ions and trienylic carbenium ions with further progress of MTO conversion (UV−vis).
(iv) Because of the absence of benzene-based carbenium ions, monoenylic carbenium ions play the key role in the early period of methanol conversion, i.e., the olefin-based reaction cycle is the dominating reaction mechanism during the early period of methanol conversion on SAPO-41.

DOI: 10.1021/jp5118757
J. Phys. Chem. C 2015, 119, 2637−2645

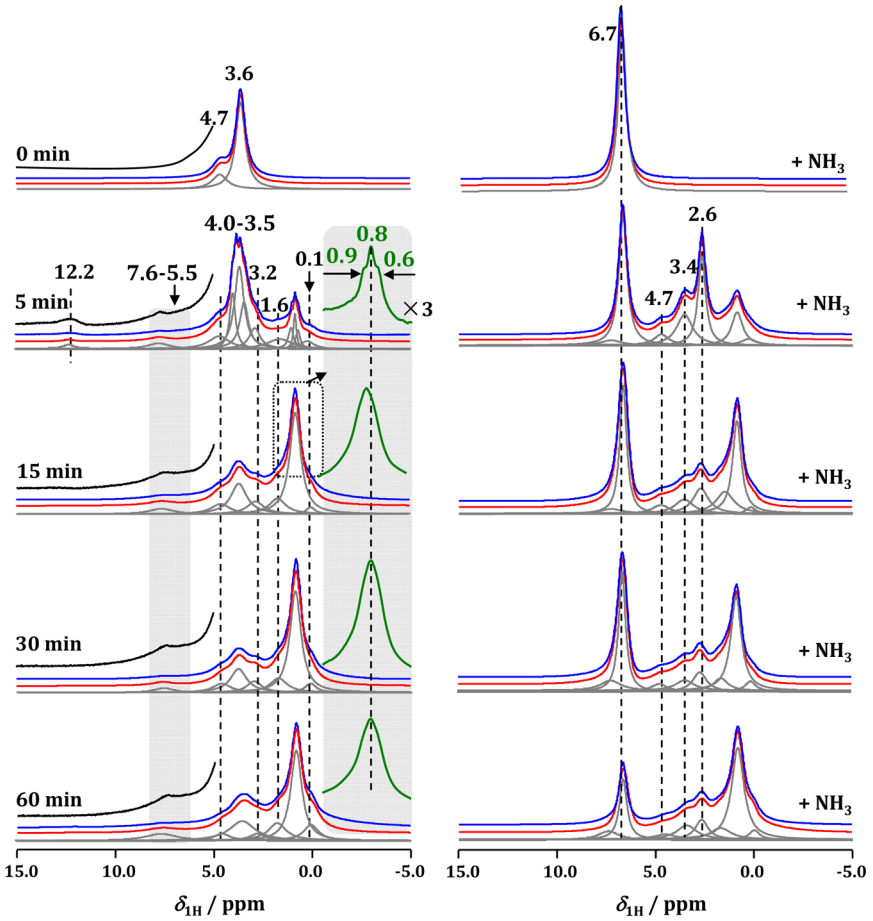

Figure 7. ^{1}H MAS NMR spectra of SAPO-41 catalysts obtained after different TOS at the reaction temperature of 350 °C and recorded before (top) and after (bottom) adsorption of ammonia. From top to bottom, experimental spectra, simulated spectra, and signal components utilized for simulation are shown.

AUTHOR INFORMATION

Corresponding Authors

*Phone/Fax: +86-22-2350-0341. E-mail: lild@nankai.edu.cn.

*Phone/Fax: +49-711-685-64081. E-mail: michael.hunger@itc.uni-stuttgart.de.

Notes

The authors declare no competing financial interest.

ACKNOWLEDGMENTS

This work was financially supported by the National Natural Science Foundation of China (21303089, 21421001), China Postdoctoral Science Foundation (2013M530870, 2014T70211), Municipal Natural Science Foundation of Tianjin (14JCQNJC05700), and Ministry of Education of China (IRT-13022). Furthermore, M.H. wants to thank the Deutsche Forschungsgemeinschaft for financial support.

REFERENCES

(1) Stöcker, M. Methanol to Olefins (MTO) and Methanol to Gasoline (MTG). In *Zeolites and Catalysis*; Cejka, J., Corma, A., Zones, S., Eds.; Wiley-VCH: Weinheim, 2010; pp 687−711.

(2) Wang, W.; Hunger, M. Reactivity of surface alkoxy species on acidic zeolite catalysts. *Acc. Chem. Res.* **2008**, *41*, 895−904.

(3) Olsbye, U.; Svelle, S.; Bjørgen, M.; Beato, P.; Janssens, T. V. W.; Joensen, F.; Bordiga, S.; Lillerud, K. P. Conversion of methanol to hydrocarbons: How zeolite cavity and pore size controls product selectivity. *Angew. Chem., Int. Ed.* **2012**, *51*, 5810−5831.

(4) Hemelsoet, K.; Mynsbrugge, J.; Wispelaere, K.; Waroquier, M.; Speybroeck, V. Unraveling the reaction mechanisms governing methanol-to-olefins catalysis by theory and experiment. *ChemPhysChem* **2013**, *14*, 1526−1545.

(5) Ilias, S.; Bhan, A. Mechanism of the catalytic conversion of methanol to hydrocarbons. *ACS Catal.* **2013**, *3*, 18−31.

(6) Dahl, I. M.; Kolboe, S. On the reaction mechanism for hydrocarbon formation from methanol over SAPO-34, 1. Isotopic labeling studies of the co-reaction of ethene and methanol. *J. Catal.* **1994**, *149*, 304−309.

(7) Dahl, I. M.; Kolboe, S. On the reaction mechanism for hydrocarbon formation from methanol over SAPO-34, 2. Isotopic labeling studies of the co-reaction of ethene and methanol. *J. Catal.* **1996**, *161*, 458−464.

(8) Arstad, B.; Kolboe, S. The reactivity of molecules trapped within the SAPO-34 cavities in the methanol to hydrocarbons reaction. *J. Am. Chem. Soc.* **2001**, *123*, 8137−8138.

(9) Song, W. G.; Haw, J. F.; Nicholas, J. B.; Heneghan, C. S. Methylbenzenes are the organic reaction centers for methanol to olefin catalysis on HSAPO-34. *J. Am. Chem. Soc.* **2000**, *122*, 10726−10727.

(10) Haw, J. F.; Song, W. G.; Marcus, D. M.; Nicholas, J. B. The mechanism of methanol to hydrocarbon catalysis. *Acc. Chem. Res.* **2003**, *36*, 317−326.

(11) Song, W. G.; Nicholas, J. B.; Sassi, A.; Haw, J. F. Synthesis of the heptamethylbenzenium cation in zeolite-*β*: In situ NMR and theory. *Catal. Lett.* **2002**, *81*, 49−53.

(12) Bjørgen, M.; Olsbye, U.; Kolboe, S. Coke precursor for mation and zeolite deactivation: Mechanistic insights from hexamethylbenzene conversion. *J. Catal.* **2003**, *215*, 30−44.

DOI: 10.1021/jp5118757
J. Phys. Chem. C 2015, 119, 2637−2645

(13) Bjørgen, M.; Olsbye, U.; Petersen, D.; Kolboe, S. The methanol-to-hydrocarbons reaction: Insight into the reaction mechanism from [12C] benzene and [13C] methanol coreactions over zeolite H-beta. *J. Catal.* **2004**, *221*, 1−10.
(14) Hemelsoet, K.; Qian, Q. Y.; Meyer, T.; Wispelaere, K.; Sterck, B.; Weckhuysen, B. M.; Waroquier, M.; Speybroeck, V. Identification of intermediates in zeolite-catalyzed reactions by in situ UV/Vis microspectroscopy and a complementary set of molecular simulations. *Chem.—Eur. J.* **2013**, *19*, 16595−16606.
(15) Song, W. G.; Fu, H.; Haw, J. F. Acid-base chemistry of a carbenium ion in a zeolite under equilibrium conditions: Verification of a theoretical explanation of carbenium ion stability. *J. Am. Chem. Soc.* **2001**, *123*, 4749−4754.
(16) Song, W. G.; Fu, H.; Haw, J. F. Selective Synthesis of Methylnaphthalenes in HSAPO-34 Cages and Their Function as Reaction Centers in Methanol-to-Olefin Catalysis. *J. Phys. Chem. B* **2001**, *105*, 12839−12843.
(17) Lesthaeghe, D.; Van der Mynsbrugge, J.; Vandichel, M.; Waroquier, M.; Van Speybroeck, V. Full Theoretical cycle for both ethene and propene formation during methanol-to-olefin conversion in H-ZSM-5. *ChemCatChem* **2011**, *3*, 208−212.
(18) Teketel, S.; Svelle, S.; Lillerud, K. P.; Olsbye, U. Shape-selective conversion of methanol to hydrocarbons over 10-Ring unidirectional-channel acidic H-ZSM-22. *ChemCatChem* **2009**, *1*, 78−81.
(19) Teketel, S.; Olsbye, U.; Lillerud, K. P.; Beato, P.; Svelle, S. Selectivity control through fundamental mechanistic insight in the conversion of methanol to hydrocarbons over zeolites. *Microporous Mesoporous Mater.* **2010**, *136*, 33−41.
(20) Li, J. Z.; Wei, Y. X.; Qi, Y.; Tian, P.; Li, B.; He, Y. L.; Chang, F. X.; Sun, X. D.; Liu, Z. M. Conversion of methanol over H-ZSM-22: The reaction mechanism and deactivation. *Catal. Today* **2011**, *164*, 288−292.
(21) Svelle, S.; Joensen, F.; Nerlov, J.; Olsbye, U.; Lillerud, K. P.; Kolboe, S.; Bjørgen, M. Conversion of methanol into hydrocarbons over zeolite H-ZSM-5: Ethene formation Is mechanistically separated from the formation of higher alkenes. *J. Am. Chem. Soc.* **2006**, *128*, 14770−14771.
(22) Bjørgen, M.; Svelle, S.; Joensen, F.; Nerlov, J.; Kolboe, S.; Bonino, F.; Palumbo, L.; Bordiga, S.; Olsbye, U. Conversion of methanol to hydrocarbons over zeolite H-ZSM-5: On the origin of the olefinic species. *J. Catal.* **2007**, *249*, 195−207.
(23) Cui, Z. M.; Liu, Q.; Song, W. G.; Wan, L. J. Insights into the mechanism of methanol-to-olefin conversion at zeolites with systematically selected framework structures. *Angew. Chem., Int. Ed.* **2006**, *45*, 6512−6515.
(24) Cui, Z. M.; Liu, Q.; Ma, Z.; Bian, S. W.; Song, W. G. Direct observation of olefin homologations on zeolite ZSM-22 and its implications to methanol to olefin conversion. *J. Catal.* **2008**, *258*, 83−86.
(25) Cui, Z. M.; Liu, Q.; Bian, S. W.; Ma, Z.; Song, W. G. The role of methoxy groups in methanol to olefin conversion. *J. Phys. Chem. C* **2008**, *112*, 2685−2688.
(26) Wei, F. F.; Cui, Z. M.; Meng, X. J.; Cao, C. Y.; Xiao, F. S.; Song, W. G. Origin of the low olefin production over HZSM-22 and HZSM-23 zeolites: External acid sites and pore mouth catalysis. *ACS Catal.* **2014**, *4*, 529−534.
(27) Ilias, S.; Bhan, A. Tuning the selectivity of methanol-to-hydrocarbons conversion on H-ZSM-5 by co-processing olefin or aromatic compounds. *J. Catal.* **2012**, *290*, 186−192.
(28) Ilias, S.; Khare, R.; Malek, A.; Bhan, A. A descriptor for the relative propagation of the aromatic- and olefin-based cycles in methanol-to-hydrocarbons conversion on H-ZSM-5. *J. Catal.* **2013**, *303*, 135−140.
(29) Erichsen, M. W.; Svelle, S.; Olsbye, U. H-SAPO-5 as methanol-to-olefins (MTO) model catalyst: Towards elucidating the effects of acid strength. *J. Catal.* **2013**, *298*, 94−101.
(30) Sun, X. Y.; Mueller, S.; Shi, H.; Haller, G. L.; Sanchez-Sanchez, M.; van Veen, A. C.; Lercher, J. A. On the impact of co-feeding aromatics and olefins for the methanol-to-olefins reaction on HZSM-5. *J. Catal.* **2014**, *314*, 21−31.
(31) Dai, W. L.; Wang, C. M.; Dyballa, M.; Wu, G. J.; Guan, N. J.; Li, L. D.; Xie, Z. K.; Hunger, M. Understanding the early stages of the methanol-to-olefin conversion on H-SAPO-34. *ACS Catal.* **2015**, *5*, 317−326.
(32) Dai, W. L.; Wang, X.; Wu, G. J.; Guan, N. J.; Hunger, M.; Li, L. D. Methanol-to-olefin conversion on silicoaluminophosphate catalysts: Effect of Brønsted acid sites and framework structures. *ACS Catal.* **2011**, *1*, 292−299.
(33) Wang, X.; Dai, W. L.; Wu, G. J.; Li, L. D.; Guan, N. J.; Hunger, M. Verifying the dominant catalytic cycle of the methanol-to-hydrocarbon conversion over SAPO-41. *Catal. Sci. Technol.* **2014**, *4*, 688−696.
(34) Buchholz, A.; Wang, W.; Xu, M. C.; Arnold, A.; Hunger, M. Thermal stability and dehydroxylation of Brønsted acid sites in silicoaluminophosphates H-SAPO-11, H-SAPO-18, H-SAPO-31, and H-SAPO-34 investigated by multi-nuclear solid-state NMR spectroscopy. *Microporous Mesoporous Mater.* **2002**, *56*, 267−278.
(35) Jiang, Y. J.; Huang, J.; Dai, W. L.; Hunger, M. Solid-state nuclear magnetic resonance investigations of the nature, property, and activity of acid sites on solid catalysts. *Solid State Nucl. Magn. Reson.* **2011**, *39*, 116−141.
(36) Deno, N. C.; Bollinger, J.; Friedman, N.; Hafer, K.; Hodge, J. D.; Houser, J. J. Carbonium ions. XIII. Ultraviolet spectra and thermodynamic stabilities of cycloalkenyl and linear alkenyl cations. *J. Am. Chem. Soc.* **1963**, *85*, 2998−3000.
(37) Kiricsi, I.; Fcrster, H.; Tasi, G.; Nagy, J. B. Generation, characterization, and transformations of unsaturated carbenium ions in zeolites. *Chem. Rev.* **1999**, *99*, 2085−2114.
(38) Jiang, Y. J.; Huang, J.; Marthala, V. R. R.; Ooi, Y.; Weitkamp, J.; Hunger, M. In situ MAS NMR-UV/Vis investigation of H-SAPO-34 catalysts partially coked in the methanol-to-olefin conversion under continuous-flow conditions and of their regeneration. *Microporous Mesoporous Mater.* **2007**, *105*, 132−139.
(39) Bjørgen, M.; Bonino, F.; Kolboe, S.; Lillerud, K.-P.; Zecchina, A.; Bordiga, S. Spectroscopic evidence for a persistent benzenium cation in zeolite H-Beta. *J. Am. Chem. Soc.* **2003**, *125*, 15863−15868.
(40) Hunger, M.; Seiler, M.; Horvath, T. A technique for simultaneous in situ MAS NMR and on-line gas chromatographic studies of hydrocarbon conversions on solidcatalysts under flow conditions. *Catal. Lett.* **1999**, *57*, 199−204.
(41) Hunger, M.; Horvath, T. Adsorption of methanol on Brønsted acid sites in zeolite H-ZSM-5 investigated by multi-nuclear solid-state NMR spectroscopy. *J. Am. Chem. Soc.* **1996**, *118*, 12302−12308.
(42) *H NMR Predictor*, Product Version 9.08; Advanced Chemistry Development Inc., Toronto, Canada, 2006.
(43) Dai, W. L.; Wang, X.; Wu, G. J.; Li, L. D.; Guan, N. J.; Hunger, M. Methanol-to-olefin conversion catalyzed by low-silica AlPO-34 with traces of Brønsted acid sites: Combined catalytic and spectroscopic investigation. *ChemCatChem* **2012**, *4*, 1428−1435.
(44) Dai, W. L.; Scheibe, M.; Guan, N. J.; Li, L. D.; Hunger, M. Fate of Brønsted acid sites and benzene-based carbenium ions during methanol-to-olefin conversion on SAPO-34. *ChemCatChem* **2011**, *3*, 1130−1133.
(45) Dai, W. L.; Scheibe, M.; Li, L. D.; Guan, N. J.; Hunger, M. Effect of the methanol-to-olefin conversion on the PFG NMR self-diffusivities of ethane and ethene in large-crystalline SAPO-34. *J. Phys. Chem. C* **2012**, *116*, 2469−2476.
(46) Dai, W. L.; Wu, G. J.; Li, L. D.; Guan, N. J.; Hunger, M. Mechanisms of the deactivation of SAPO-34 materials with different crystal sizes applied as MTO catalysts. *ACS Catal.* **2013**, *3*, 588−596.
(47) Jiang, Y. J.; Hunger, M.; Wang, W. On the reactivity of surface methoxy species in acidic zeolites. *J. Am. Chem. Soc.* **2006**, *128*, 11679−11692.
(48) *C NMR*, Version 1.1, Advanced Chemistry Development Inc., Toronto, Canada, 1995.
(49) Goguen, P.; Xu, T.; Barich, D.; Skloss, T.; Song, W. G.; Wang, Z.; Nicholas, J.; Haw, J. F. Pulse-quench catalytic reactor studies reveal

DOI: 10.1021/jp5118757
J. Phys. Chem. C 2015, 119, 2637−2645

a carbon-pool mechanism in methanol-to-gasoline chemistry on zeolite HZSM-5. *J. Am. Chem. Soc.* **1998**, *120*, 2650−2651.
(50) Olah, G. A.; Liang, G. Stable carbocations. CXXXVII. Cycloheptenyl, cyclooctenyl, and cyclononenyl cations. *J. Am. Chem. Soc.* **1972**, *94*, 6434−6441.

DOI: 10.1021/jp5118757
J. Phys. Chem. C 2015, 119, 2637−2645